

## Anomalies of linewidth and intensity in the reorientation spectra of a critical mixture

D. Beysens and G. Zalczer

*Commissariat à l'Énergie Atomique, Service de Physique du Solide et de Résonance Magnétique,  
Centre d'Études Nucleaires de Saclay, Boîte Postale No. 2, 91190 Gif-sur-Yvette, France*

(Received 30 November 1977)

The critical behavior of the depolarized Rayleigh spectrum in the system nitrobenzene-*n*-hexane has not been previously accurately assessed because in usual Fabry-Pérot experiments the multiple-scattering contribution completely overwhelms the spectrum within a few degrees of the critical temperature  $T_c$ . By using a high-performance double-pass Fabry-Pérot interferometer, we have been able to obtain accurate measurements of both linewidth and intensity, from 50°C to temperatures as close as 0.026°C to  $T_c$ . Two lines due to nitrobenzene molecules in solution are visible. The first line (1) is intense and narrow, while the second line (2) is weak and broad. The spectral intensity of (2) is about  $10^{-2}$  times that of (1). The linewidth of (1) is seen to behave as the inverse shear viscosity, with a critical divergence with exponent  $Y \approx 0.04$ . The intensity of (1) exhibits a power-law divergence with exponent  $\Omega \approx 0.2$ . These results are compared with data obtained in pure nitrobenzene and *n*-hexane, and in noncritical mixtures of nitrobenzene.

### I. INTRODUCTION

Depolarized light scattering has previously been widely used to study short-range effects in liquids<sup>1-4</sup> and in liquid mixtures.<sup>5,6</sup> However, it is only recently that this technique has been applied to binary mixtures near their critical point by Fabelinskiĭ *et al.*,<sup>7-10</sup> followed by Aref'ev<sup>11</sup> and ourselves.<sup>12</sup>

The results obtained in this field strongly disagree with each other: Fabelinskiĭ *et al.* found a strong anomaly in the width of the reorientation lines, whereas other measurements are compatible with at most a weak anomaly related to the behavior of the shear viscosity near the transition point.<sup>13</sup> This discrepancy can be explained on purely experimental grounds,<sup>14</sup> as Fabelinskiĭ *et al.* did not take sufficient account of multiple scattering, which in most critical mixtures becomes very important near the transition temperature ( $T_c$ ).

In any case, the behavior of the reorientation lines close to  $T_c$  cannot be inferred from the existing results. Moreover, the variation of the corresponding intensities is not well understood.<sup>12</sup> The present work consequently tries to answer the following questions: (i) Are there several depolarized lines? (ii) Is there a strong, weak, or in fact no anomaly at all in the behavior of both the linewidth and intensity of this (these) line(s)? (iii) More precisely, is the close relation generally observed between the shear viscosity and the reorientation linewidth still valid near  $T_c$ ?

We chose for this study the binary mixture of nitrobenzene and *n*-hexane. Indeed, the molecules of nitrobenzene are very anisotropic, giving rise

to an intense depolarized scattering, and they have a high permanent dipole moment which is a possible source of strong orientation correlations (orientational local order). Furthermore, nitrobenzene has been widely studied by light scattering, both neat and in solution. *n*-hexane is nonpolar, weakly anisotropic, and plays the role of an isotropic solvent. Moreover, this critical mixture has been studied in great detail near  $T_c$  by many authors.<sup>15-20</sup>

On the other hand, since the refractive indices of the components are very different, multiple scattering occurs near  $T_c$ , so that a high-performance setup is required. With a double-pass Fabry-Perot (FP) interferometer with variable thickness, which allows the multiple-scattering line to be separated from other depolarized contributions, we could obtain intensity and linewidth measurements in the frequency range 2-400 GHz and in the temperature range  $T - T_c = 0.026-50$  °C. We show that there are two lines present, which is also the case in pure nitrobenzene.<sup>21</sup> The first line is a sharp and intense Lorentzian with a linewidth behaving roughly like the inverse viscosity, while the corresponding intensity approximately diverges with a power law (exponent  $\Omega \approx 0.22$ ). The second line is nearly 15 times broader with an intensity seven times lower, thus the spectral intensity is so weak that it is no longer detectable when  $T - T_c$  is smaller than a few degrees.

### II. EXPERIMENTAL

The liquids used were of spectroscopic grade and filtered through 0.2- $\mu$ m Teflon filters in order to remove dust particles. The binary mixture has

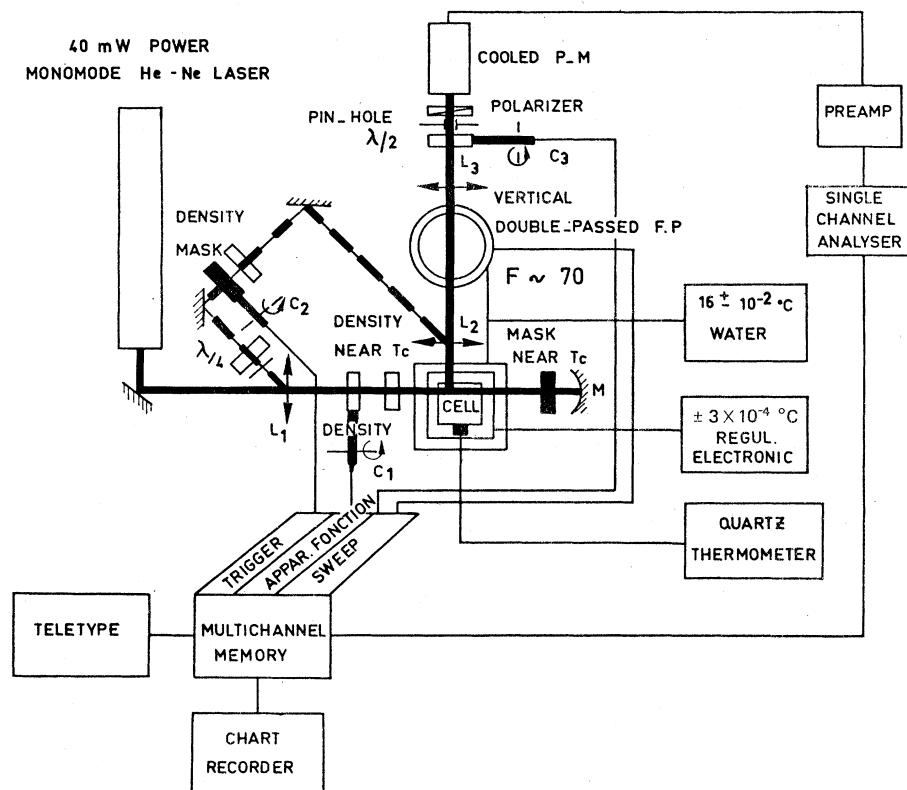


FIG. 1. General description of the setup.  $L_1$ ,  $L_2$ , and  $L_3$  are lenses;  $C_1$ ,  $C_2$ , and  $C_3$  are choppers.

a critical concentration of 0.51 wt% of nitrobenzene (0.42 mol%).<sup>15</sup> The experimental concentration was  $0.509 \pm .002$ , and the meniscus appeared in the middle of the cell, which is a good test for verifying the critical concentration. The temperature is measured by means of a quartz thermometer allowing relative measurements to be performed with a resolution of  $10^{-4} \text{ }^\circ\text{C}$ . Precise absolute-temperature measurements were not required ( $T_c \approx 20 \text{ }^\circ\text{C}$ ). The sample was located in a copper oven, itself inside a thermally regulated box. The temperature fluctuation was less than  $5 \cdot 10^{-4}$  over more than 24 h.

The detailed description of the spectrometer and its operation can be found in Ref. 22. The main features are (see Fig. 1): (i) A plane double-pass FP interferometer, working in a vertical position, which gives a passive stability allowing experiments to be continued over more than 24 h. The FP interferometer is placed in an air-tight box at a constant temperature and is piezoelectrically scanned. The spacing between the plates is variable and we used two different free spectral ranges (FSR), 78 GHz and 1087 GHz. The plates that we used give a contrast better than  $10^6$ , a finesse of 70, and a transmission of

5% with a 2-cm useful aperture. (ii) A He-Ne laser ( $\lambda = 6328 \text{ \AA}$ ) as incident light, monomode (40 mW power) when a 78 GHz FSR was used. (iii) Quasisimultaneous recording of both the apparatus function (AF) and the spectrum, by sequences of 9 spectra ( $9 \times 2 \text{ sec}$ ) and one AF (2 sec) over a time period up to 48 h. The AF was provided by the very intense low-frequency ( $\sim 1 \text{ KHz}$ ) polarized spectrum. (iv) Automatic compensation of frequency drifts of the laser line. (v) Photon counting (maximum rate  $5 \times 10^5 \text{ sec}^{-1}$ ).

A Glan prism selects the VH polarization when the spectrum is recorded. A half-wave plate rotates the polarization of the detected light by  $\frac{1}{2}\pi$  when the AF is recorded.

In order to minimize the effects of both turbidity<sup>23</sup> and multiple scattering,<sup>18,19</sup> the scattering volume was set close to the entrance and exit windows. Near  $T_c$ , we had to attenuate the incident beam strongly (up to 1.3 mW) in order, first, to avoid extra heating of the sample, and second, to maintain the scattered light (dominated by the multiple scattering) below the saturation level of the counting chain. Therefore, close to  $T_c$  recording times longer than 24 h are necessary in order to obtain a reasonable signal-to-noise ratio.

A program of statistical refining, due to Tournarie,<sup>24</sup> determines the best fit of the experimental spectrum. The "quality" of the fit is measured by a coefficient  $Q$ , which gives the contribution of the statistical error to the total deviation: A purely random deviation would give  $Q = 1$ , whereas a systematic distortion drastically lowers  $Q$ .

Figure 2 shows a spectrum with a FSR of 1087 GHz. A weak, broad line can be detected, as in pure nitrobenzene,<sup>21</sup> in addition to a central peak which contains at least a narrow line plus an AF. The fitting program failed when the convolution product of the AF by only one Lorentzian line plus a Dirac function, due to the quasielastic scattering (both polarized scattering and multiple scattering), was considered. So we fitted the experimental spectra to an AF plus two Lorentzian lines, representing the convolution of the AF by a true spectrum composed of a Dirac function and two Lorentzian lines. Of course, correction of half-widths and overlapping from neighboring interferometer orders were taken into account. We tried also an exponential shape for the broad line, which gave a fit as good as that previously obtained, with a characteristic frequency of the same order of magnitude. It is worth noticing that a simple fit of only the wings of the spectrum to one single line gives quite different results, showing that the wings of the narrow line cannot be neglected.

Figure 3 shows two spectra at two temperatures

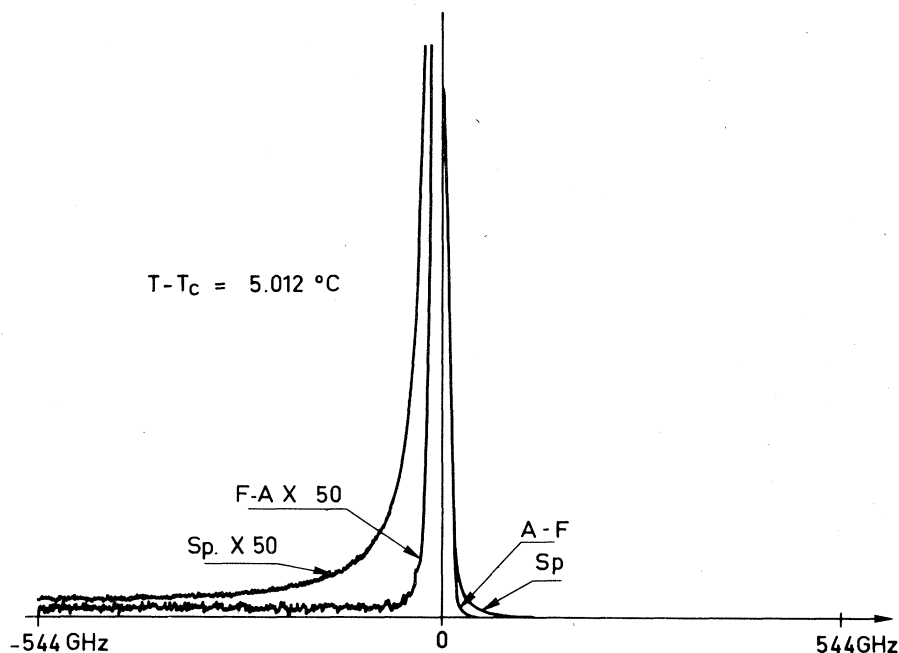


FIG. 2. Total spectrum with a FSR of 1087 GHz at two different scales showing (right) the narrow spectrum plus a strong AF (quasielastic scattering), and (left) the broad spectrum.

with a FSR of 78 GHz, i.e., much smaller than the former FSR. These spectra have been successfully analyzed (Fig. 4) by considering them as the convolution product of the AF by a true spectrum composed of a flat background (nonresolved lines), a Lorentzian line (anisotropy line), and a Dirac function accounting for the quasielastic scattering, as in pure nitrobenzene.

The linewidths obtained in the computing programs are expressed in units of FSR, which itself can be measured with an accuracy of about 1%. The final uncertainty is near 5%.

The numbers  $I_1^*$ ,  $I_2^*$ ,  $D^*$ , and  $P^*$  given by the computer for the intensities of, respectively, the narrow and wide Lorentzian lines, the quasielastic depolarized scattering, and the polarized scattering, are meaningless unless corrected by many factors, such as laser intensity, turbidity, FP interferometer transmission, aperture angles, etc. However, the ratios of these numbers, for a given recording, are automatically corrected for all these factors; thus the variations of the true intensities  $I_1$ ,  $I_2$ ,  $D$ , and  $P$  can be deduced from the variations of one of them. Obviously, the polarized scattering intensity  $P$  is the best known,<sup>19,20</sup>

$$P(T - T_c) \propto \frac{T}{T_c} \frac{(T - T_c)^{-1.22}}{1 + 0.0286(T - T_c)^{-1.22}}.$$

So we get  $I_{1,2} = (I_{1,2}^*/P^*)P$ . This method has been used for the set of experiments  $\alpha$  in Table I. Typical uncertainties are 8%.

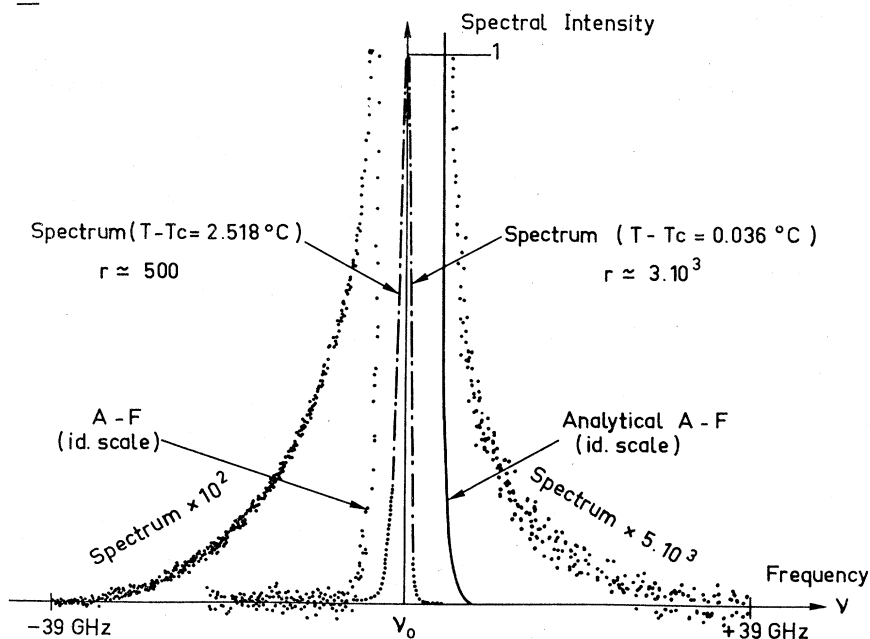


FIG. 3. Typical narrow spectra with the same reduced scale. The AF are shown with the same spectral intensity at frequency  $\nu_0$ . Both experimental and analytical AF are shown.  $r$  is the ratio of spectral intensities (peak/line) at frequency  $\nu_0$ .

In set  $\beta$  of Table I,  $P^*$  could not be accurately measured, so we calibrated the intensity by the depolarized quasielastic scattering  $D^*$ . A difficulty with this method is that the spatial variation

around the exciting beam is not the same as the polarized or depolarized single scattering.<sup>18</sup> Nevertheless, since the set  $\beta$  was performed in the same experimental conditions as the set  $\alpha$ , we

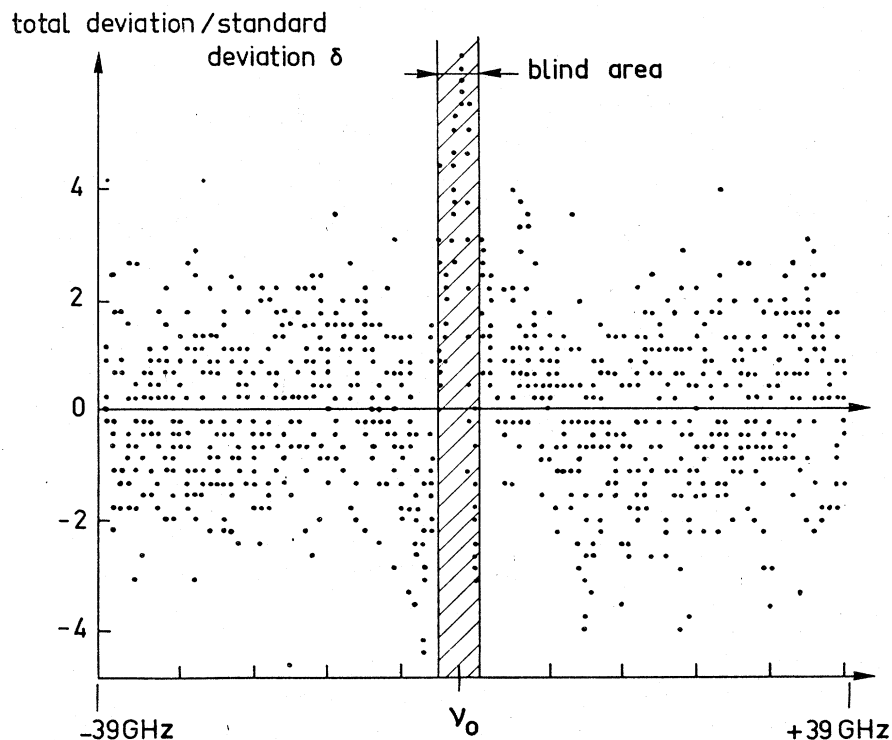


FIG. 4. Reduced deviation vs frequency for a narrow spectrum recorded at  $T-T_c=0.0290$  °C with a ratio of spectral intensities  $r \approx 5000$ . The quality coefficient is  $Q=0.54$ , due to the distortions in the "blind" region where the peak is situated.

can infer from set  $\alpha$  the experimental ratio

$$D^*/P^* = a + bP(T - T_c),$$

$$a = 19.1 \pm 0.5, \quad b = (9.4 \pm 1.4) \times 10^{-2}.$$

The first term ( $a$ ) is due to polarizer defects, the second ( $b$ ) arises from double scattering and depends on the actual experimental geometry.

From the computed intensity  $I^*$  it is then straightforward to obtain

$$I(T - T_c) = \frac{I^* D^*}{D^* P^*} P(T - T_c)$$

$$= \frac{I^*}{D^*} [aP(T - T_c) + bP^2(T - T_c)].$$

The results for set  $\beta$  can be found in Table I. Typical uncertainties are 12%.

We also give in Table I early (graphical) published experiments<sup>12</sup> (set  $\gamma$ ) where the intensity was referred to the incident power. Both FP

TABLE I. Measurements for sets  $\alpha$ ,  $\beta$ , and  $\gamma$ .

Set $\alpha$			Set $\beta$		
$(T/T_c) - 1$	$\tau_1 (\times 10^{-12} \text{s})$	$I_1 \pm 10\%$	$(T/T_c) - 1$	$\tau_1 (\times 10^{-12} \text{s})$	$I_1 \pm 12\%$
$1.31 \times 10^{-1}$	$9.87 \pm 0.26$	4.67	$7.66 \times 10^{-2}$	$11.9 \pm 1$	6.6
$1.211 \times 10^{-1}$	$10.45 \pm 0.32$	4.90	$7.66 \times 10^{-2}$	$12.7 \pm 1$	
$1.03 \times 10^{-1}$	$9.97 \pm 1.4$	5.49	$5.1 \times 10^{-2}$	$14.8 \pm 1.3$	7.91
$8.57 \times 10^{-2}$	$10.82 \pm 0.32$	6.38	$3.5 \times 10^{-2}$	$15.3 \pm 1.1$	9.60
$6.04 \times 10^{-2}$	$11.9 \pm 2.1$	7.19	$2.7 \times 10^{-2}$	$14.6 \pm 1.1$	7.01
$5.05 \times 10^{-2}$	$15.2 \pm 0.45$	7.25	$2.32 \times 10^{-2}$	$15.3 \pm 1.1$	12.6
$3.72 \times 10^{-2}$	$12.4 \pm 0.32$	6.40	$1.63 \times 10^{-2}$	$17.4 \pm 1.3$	9.95
$3.36 \times 10^{-2}$	$12.6 \pm 0.53$	8.23	$1.50 \times 10^{-2}$	$15.7 \pm 1.1$	9.24
$1.99 \times 10^{-2}$	$14.2 \pm 2.75$	9.01	$1.50 \times 10^{-2}$	$16.3 \pm 1.3$	
$1.54 \times 10^{-2}$	$15.6 \pm 0.48$	7.04	$1.09 \times 10^{-2}$	$13.5 \pm 4.5$	11.7
$9.54 \times 10^{-3}$	$15.2 \pm 0.45$	9.54	$8.97 \times 10^{-3}$	$16.5 \pm 1.3$	13.9
$8.594 \times 10^{-3}$	$15.6 \pm 0.32$	10.8	$6.18 \times 10^{-3}$	$16.1 \pm 1.3$	10.9
$5.78 \times 10^{-3}$	$16.9 \pm 0.32$	11.8	$3.77 \times 10^{-3}$	$16.1 \pm 2.4$	13.2
$5.017 \times 10^{-3}$	$16.07 \pm 0.32$	14.5	$3.47 \times 10^{-3}$	$15.7 \pm 1.1$	11.3
$3.778 \times 10^{-3}$	$16.07 \pm 0.32$	13.7	$3.2 \times 10^{-3}$	$15.0 \pm 2.4$	14.0
$2.43 \times 10^{-3}$	$17.0 \pm 3.2$	13.3	$2.9 \times 10^{-3}$	$16.4 \pm 1.1$	14.1
$1.66 \times 10^{-3}$	$17.4 \pm 0.48$	7.79	$2.58 \times 10^{-3}$	$16.3 \pm 1.1$	15.5
$1.177 \times 10^{-3}$	$16.07 \pm 0.53$	13.6	$2.3 \times 10^{-3}$	$16.5 \pm 1.1$	17.5
$8.055 \times 10^{-4}$	$14.1 \pm 0.48$	13.7	$1.7 \times 10^{-3}$	$16.8 \pm 1.1$	18.5
$4.73 \times 10^{-4}$	$16.87 \pm 0.37$	30.8	$1.7 \times 10^{-3}$	$16.9 \pm 1.1$	16.1
$4.266 \times 10^{-4}$	$18.46 \pm 0.58$	18.5	$1.37 \times 10^{-3}$	$16.6 \pm 1.1$	20.5
$3.53 \times 10^{-4}$	$19.0 \pm 0.69$	15.4	$1.0 \times 10^{-3}$	$18.0 \pm 1.1$	25
$2.96 \times 10^{-4}$	$17.7 \pm 0.42$	22.5	$9.3 \times 10^{-4}$	$19.1 \pm 1.5$	20.9
$2.64 \times 10^{-4}$	$18.7 \pm 1$	25.1	$8.43 \times 10^{-4}$	$18.7 \pm 6.3$	24.8
$2.59 \times 10^{-4}$	$20.1 \pm 0.70$	...	$5.7 \times 10^{-4}$	$18.0 \pm 1.5$	26.6
$2.33 \times 10^{-4}$	$17.88 \pm 0.37$	24.7	$5.0 \times 10^{-4}$	$20.0 \pm 1.6$	26.0
$1.79 \times 10^{-4}$	$20.9 \pm 0.50$	19.1	$2.7 \times 10^{-4}$	$18.0 \pm 1.3$	29.7
$1.706 \times 10^{-4}$	$15.7 \pm 0.53$	26.6			
$1.481 \times 10^{-4}$	$13.05 \pm 2.6$	27.8			
$1.365 \times 10^{-4}$	$20.9 \pm 1.3$	26.1			
$1.27 \times 10^{-4}$	$27.00 \pm 1.6$	21.3			
$1.229 \times 10^{-4}$	$18.3 \pm 0.58$	27.0			
$9.9 \times 10^{-5}$	$17.2 \pm 0.58$	22.9			
$8.87 \times 10^{-5}$	$20.90 \pm 4.1$	27.4			

TABLE I. (Continued)

Set $\gamma$					
$(T/T_c) - 1$	$\tau_1(10^{-12} \text{ sec}) \pm 10\%$	$I_1 \pm 12\%$	$(T/T_c) - 1$	$\tau_1(10^{-12} \text{ sec}) \pm 10\%$	$I_1 \pm 12\%$
$1.73 \times 10^{-1}$	9.92	2.90	$2.9 \times 10^{-2}$	16.4	4.25
$1.65 \times 10^{-1}$	8.86	2.85	$2.76 \times 10^{-2}$	13.6	
$1.61 \times 10^{-1}$	8.86	1.54	$2.72 \times 10^{-2}$	15.4	
$1.54 \times 10^{-1}$	9.92	2.35	$2.70 \times 10^{-2}$	14.0	
$1.46 \times 10^{-1}$	10.0	2.45	$2.55 \times 10^{-2}$	15.6	4.35
$1.38 \times 10^{-1}$	9.8	2.70	$2.50 \times 10^{-2}$	15.3	5.20
$1.35 \times 10^{-1}$	8.9	3.70	$2.13 \times 10^{-2}$	16.4	
$1.31 \times 10^{-1}$	10.3	2.55	$2.04 \times 10^{-2}$	14.8	
$1.28 \times 10^{-1}$	10.0	3.30	$2.00 \times 10^{-2}$	13.5	
$1.23 \times 10^{-1}$	10.8	4.05	$2.00 \times 10^{-2}$	14.7	4.75
$1.20 \times 10^{-1}$	9.9	2.85	$1.98 \times 10^{-2}$	15.2	5.00
$1.18 \times 10^{-1}$	11.0		$1.90 \times 10^{-2}$	15.2	4.75
$1.18 \times 10^{-1}$	10.0	3.85	$1.90 \times 10^{-2}$	16.8	4.80
$1.05 \times 10^{-1}$	11.3	3.05	$1.60 \times 10^{-2}$	16.8	
$1.01 \times 10^{-1}$	10.6	4.05	$1.40 \times 10^{-2}$	16.2	4.80
$9.41 \times 10^{-2}$	11.5	3.25	$1.40 \times 10^{-2}$	19.5	4.80
$8.82 \times 10^{-2}$	11.7	3.85	$1.38 \times 10^{-2}$	18.5	
$7.86 \times 10^{-2}$	12.7	3.60	$1.14 \times 10^{-2}$	16.9	
$6.73 \times 10^{-2}$	13.3	3.95	$1.13 \times 10^{-2}$	19.3	5.40
$6.25 \times 10^{-2}$	13.7	3.50	$1.10 \times 10^{-2}$	19.7	5.55
$5.70 \times 10^{-2}$	12.4	5.10	$1.04 \times 10^{-2}$	17.7	5.15
$5.06 \times 10^{-2}$	15.2	4.20	$9.89 \times 10^{-3}$	a	5.20
$4.4 \times 10^{-2}$	12.9	4.40	$8.19 \times 10^{-3}$	...	4.95
$4.23 \times 10^{-2}$	13.5	4.95	$7.51 \times 10^{-3}$	...	5.20
$4.13 \times 10^{-2}$	12.9	3.9	$6.48 \times 10^{-3}$	...	5.10
$4.02 \times 10^{-2}$	15.3		$6.48 \times 10^{-3}$	...	5.40
$3.98 \times 10^{-2}$	12.8		$5.80 \times 10^{-3}$	...	5.00
$3.85 \times 10^{-2}$	13.5		$4.78 \times 10^{-3}$	...	5.60
$3.84 \times 10^{-2}$	14.2		$3.75 \times 10^{-3}$	...	6.00
$3.83 \times 10^{-2}$	14.2		$3.75 \times 10^{-3}$	...	5.10
$3.49 \times 10^{-2}$	15.6	4.60	$2.73 \times 10^{-3}$	...	4.60
$3.41 \times 10^{-2}$	13.8	4.05			
$3.37 \times 10^{-2}$	14.0				
$3.36 \times 10^{-2}$	16.6				
$3.36 \times 10^{-2}$	16.6				
$3.24 \times 10^{-2}$	14.0				
$3.17 \times 10^{-2}$	13.1				
$3.05 \times 10^{-2}$	14.9				

<sup>a</sup>  $\tau_1$  accuracy is much worse than the  $I_1$  accuracy in the range  $T - T_c = 1 - 3^\circ\text{C}$ .

interferometer transmission and turbidity were nearly constant in this experiment (single-pass FP interferometer,  $T - T_c > 1^\circ\text{C}$ ).

### III. EXPERIMENTAL RESULTS

#### A. Pure components

*n* hexane is a quasi-isotropic solvent. A depolarized spectrum recorded with a FSR of 1087

GHz shows a line of about 20 GHz, which is probably the Rayleigh-Brillouin components broadened by the aperture angle: the ratio of the depolarized intensity to the polarized intensity is of the order of magnitude of  $10^{-3}$ , i.e., the polarization ratio.

Nitrobenzene exhibits two lines of half-width (at  $T = 20^\circ\text{C}$ )  $\Gamma_1 = 5, 50 \text{ GHz}^2$  and  $\Gamma_2 \approx 300 \text{ GHz}$ .<sup>21</sup> The first line (1) is a sharp and intense Lorent-

zian which shows when resolved a structure due to a coupling with shear waves.<sup>25</sup> This phenomenon, the unusual weak value of the linewidth, and the high corresponding intensity, suggest a strong local-orientation order. The temperature variation of the intensity<sup>2</sup> is roughly linear but much more important than the density variation. The second line (2) is weak and broad: the ratio of intensities  $I(2)/I(1) \approx \frac{1}{20}$ ,<sup>21</sup> so that the ratio of spectral intensities is weaker by about  $\sim 10^{-3}$ . This fact explains the polemic about its existence, since a contrast of much more than  $10^3$  is needed, which is rather difficult to obtain with a single-pass FP interferometer. The first line has a temperature dependence like the inverse viscosity following an Arrhenius law with activation energy of  $2.4 \times 10^{-13}$  erg.<sup>2,4</sup> The temperature dependence of the second line has not been investigated.

We neglect, of course, the influence of broader lines related to anisotropy-induced effects (linewidth  $\sim 10^3$  GHz),<sup>26</sup> inertial phenomena, etc. These lines cannot be seen in the FSR of 78 and 1087 GHz. The following discussion will therefore refer to the two lines of nitrobenzene in solution with *n* hexane. Nevertheless, before considering the critical mixture, let us recall some results concerning noncritical mixtures of nitrobenzene in isotropic or quasi-isotropic solvents.

#### B. Noncritical mixtures of nitrobenzene

We will be chiefly concerned with spectrum (1). A study of nitrobenzene in carefully chosen solvents enables the variation of  $\Gamma_1$  or  $\tau_1 = (1/2\pi\Gamma_1)$  with the shear viscosity ( $\eta_s$ ) and/or the volume percent ( $x$ ) of nitrobenzene to be examined. The following empirical formula was found by Alms *et al.*,<sup>6</sup> where  $u$  and  $\tau_0$  are empirical functions of  $x$

$$\tau_1(x, \eta) = u(x)\eta + \tau_0(x). \quad (1)$$

The temperature dependence was not investigated ( $T \approx 24^\circ\text{C}$ ). The solvent seems to have no action on the reorientation time, the meaningful parameters being the concentration and the viscosity. Nevertheless, the signification of  $\tau_0(x)$  is not clear; it could be related to inertial effects due to dilution, i.e., an influence of the molecules of the solvents.

The intensity is strongly correlated to the dilution following the variation with  $N$ , the number of molecules per unit volume,

$$I_1(N) \propto N(1+fN),$$

where  $f$  is a parameter related to the strength of local static orientation correlations. Its value is close to 1; this means roughly that in neat nitro-

benzene, several molecules cooperatively scatter. And for the concentration  $x = x_c$ , one finds:  $I_1(x_c)/I_1(1) \approx 0.22$  following Refs. 5 and 6.

The variations of the time  $\tau_1$  and of the corresponding intensity  $I_1$  seem to indicate the presence of a strong local-orientational order, which decreases with increasing dilution, to reach a "monomolecular" scattering at infinite dilution. To our knowledge, the behavior of both the reorientation time  $\tau_2$  and the intensity  $I_2$  have not been previously investigated. We will now consider the behavior of these two lines in a critical mixture.

#### C. Critical mixture nitrobenzene *n* hexane

##### 1. Broad line

As we have already pointed out, the analysis of this line, with weak spectral intensity, in the presence of strong quasielastic scattering and a narrow depolarized spectrum, with the presence of non-negligible overlapping from neighboring interferometer orders, is not easy. So we cannot expect very accurate results, and did not investigate this line extensively. Four spectra, at  $T - T_c = 0.1, 1, 5,$  and  $12^\circ\text{C}$ , were recorded. Due to the drastic increase of the quasielastic scattering near  $T_c$ , at  $T - T_c = 0.1^\circ\text{C}$  the broad line is no longer visible. In the range  $12-1^\circ\text{C}$ , the linewidth is nearly constant:  $\Gamma_2 \approx 145$  GHz. We will further see that this linewidth corresponds at  $T - T_c = 1^\circ\text{C}$  to the ratio between the broad and narrow linewidths

$$\Gamma_2/\Gamma_1 \approx 15.$$

The ratio of the intensities is nearly

$$I_2/I_1 \approx 0.15.$$

So, the spectral intensity of the broad line is therefore about 1% of the narrow line. These results ensure that the broad line appears as a weak and flat background when a FSR of 78 GHz is used.

##### 2. Narrow line: Study of the linewidth

The results for three sets of experiments can be found in Table I: (i) set  $\alpha$ :  $T - T_c = 0.026-40^\circ\text{C}$ ; (ii) set  $\beta$ :  $T - T_c = 0.1-25^\circ\text{C}$ . These data concern preliminary measurements performed with a nonmonomode laser. (iii) set  $\gamma$ :  $T - T_c = 3-50^\circ\text{C}$ . These measurements (in the range  $1-50^\circ\text{C}$ ) have been already published in Figs. 3 and 4 of Ref. 12. They were performed with a single-pass FP interferometer and a nonmonomode laser. Following a previous analysis,<sup>14</sup> we suppress the range  $1-3^\circ\text{C}$  where the uncertainties

were much bigger.

We tried first to compare our data to Eq. (1), i.e., at  $T = 24^\circ\text{C}$ , and for the viscosity and concentration of the critical mixture:

$$x = x_c = 0.42 \text{ mol } \%$$

$$u(x_c) \approx 8.75 \cdot 10^{-12} \text{ sec } cP_0^{-1} \text{ (Ref. 6),}$$

$$\tau_0(x_c) \approx 7.5 \cdot 10^{-12} \text{ sec (Ref. 6),}$$

$$\eta_s^c(24^\circ\text{C}) \approx 0.585 cP_0 \text{ (Ref. 13).}$$

Equation (1) gives a reorientation time of

$$\tau_1(x = x_c, \eta_s = \eta_s^c, T = 24^\circ\text{C}) \approx 12.6 \times 10^{-12} \text{ sec,}$$

whereas our measurements give a mean value of about

$$\tau_1(\text{experimental}) \approx 16.2 \times 10^{-12} \text{ sec.}$$

The agreement is therefore reasonable, and one could expect a weak influence from the critical properties on the reorientation time.

Second, we tried to fit Eq. (1) to our linewidth data,  $\eta_s$  being considered as a variable (function of  $T - T_c$ ), and  $u$  and  $\tau_0$  being the adjustable parameters, called  $u^*$  and  $\tau_0^*$ . The values of  $\eta_s$  are inferred from shear viscosity measurements of Ref. 13 performed close to  $T_c$  and which exhibit the usual critical anomaly, i.e., an increase of about 20% near  $T_c$

$$\eta_s^c = \eta_0 \exp\left(\frac{E}{kT}\right) \left(\frac{T - T_c}{T_c}\right)^{-Y}, \quad (2)$$

where  $\eta_0 = (143 \pm 5) \times 10^{-6} P_0$ , and  $E = (1.450 \pm 0.016) \times 10^{-13}$  erg;  $Y = 0.0430 \pm 3.10^{-4}$  is a critical exponent.  $k$  is the Boltzmann constant.

The results of the fit are shown in Table II, where we can see that the statistical quality is quite good, justifying Eq. (1). Nevertheless,  $\tau_0^*$  is found to be negligible small, whereas  $u^*$  is significantly bigger than  $u(x_c)$  [indeed, at  $24^\circ\text{C}$ ,  $u(x_c)\eta_s^c + \tau_0(x_c) \approx u^*\eta_s^c$ ]. Therefore, either both  $u(x_c)$  and  $\tau_0(x_c)$  have a strong temperature dependence, at least of the same order of magnitude as the viscosity and there is no meaningful information to be drawn from this comparison, or  $\tau_0$  is a function of the solvent, and its influence

TABLE II. Fit to  $\tau_1 = u^*\eta_s^c + \tau_0^*$

Set	$u^*$ ( $10^{-12} \text{ sec} \cdot c P_0^{-1}$ ) $\pm \Delta u^*$	$\tau_0^*$ ( $10^{-12} \text{ sec}$ ) $\pm \Delta \tau_0^*$	$Q$		
$\alpha$	22.6	1.7	1.7	1	0.99
$\beta$	20.0	4	4.6	2.4	0.77
$\gamma$	27.8	0.4	0.01	0.05	0.98
$\alpha + \beta + \gamma$	21.9	0.7	2.5	0.5	0.83

TABLE III.

Fit	Set	$\tau_1^*$ ( $10^{-12} \text{ sec}$ )	$\tau_1^* \exp(E_1^*/1 + \epsilon) \epsilon^{-Y_1}$ $\pm \Delta \tau_1^*$ ( $10^{-12} \text{ sec}$ )	$E_1^*$ $\pm \Delta E_1^*$	$Y_1$ $\pm \Delta Y_1$	$Q$	$\delta$ (Ref. b)	$Q$	$\delta$ (Ref. b)
$\alpha$	Y free	0.50	0.3	3.3	0.7	0.036	0.01	0.99	0.9
	Y=0	0.10	0.05	5.2	0.5	0	0	0.81	1
$\beta$	Y free	0.77	0.8	3.0	1	0.025	0.015	0.64	1
	Y=0	0.17	0.09	4.6	0.6	0	0	0.52	1
$\gamma$	Y free	1.2	1	2	1	0.1	0.06	0.80	0.8
	Y=0	0.15	0.05	4.7	0.3	0	0	0.96	1
$\alpha + \beta + \gamma$	Y free	0.41	0.12	3.56	0.3	0.030	0.005	0.94	0.9
	Y=0	0.12	0.03	4.99	0.25	0	0	0.83	1

<sup>b</sup> $\delta$ : reduced standard deviation (for each set).

<sup>a</sup> $\epsilon = (T - T_c)/T_c$ .



would be negligible in this particular mixture.

The reorientation time seems to behave as the inverse viscosity with its critical behavior. A more sensitive test is to fit the data to the same critical variation (2) found for the viscosity

$$\tau_1 = \tau_1^0 \exp\left(\frac{E_1^0}{kT}\right) \left(\frac{T - T_c}{T_c}\right)^{-Y_1^0} \quad (3)$$

$\tau_1^0$ ,  $E_1^0$ , and  $Y_1^0$  are adjustable parameters. In order to assess the point that the very weak exponent  $Y_1^0$  is well determined, we fit also the data with  $Y_1^0 = 0$ .

Table III shows the results. One can notice that (i) the quality  $Q$  of the fit increases when  $Y_1^0 \neq 0$ , (ii) the reduced standard deviation  $\delta$  decreases when  $Y_1^0 \neq 0$ , (iii) the activation energy  $E_1^0$  is quite different from the shear viscosity activation energy when  $Y_1^0 = 0$  is assumed.

It is obvious that the best measurement of  $Y$  is performed in set  $\alpha$  where the data are closest to  $T_c$ . The corresponding parameters of both the shear viscosity and the reorientation time are nearly identical. We have for set  $\alpha$ :

$$E_1^0/E = 0.9 \pm 0.2, \quad Y_1^0/Y_1 = 0.84 \pm 0.3,$$

and for sets  $\alpha + \beta + \gamma$ :

$$E_1^0/E = 1.00 \pm 0.08, \quad Y_1^0/Y = 0.7 \pm 0.2.$$

In Fig. 5 are shown sets  $\alpha$ ,  $\beta$ , and  $\gamma$  with these

last values.

It is also convenient to compare the reorientation time with the viscosity divided by  $T$ , following an hydrodynamic model of rotation (Brownian model of rotation). The following formula has been tested

$$\tau_1 = \tau_1^1 \frac{1}{T} \exp\left(\frac{E_1^1}{kT}\right) \left(\frac{T - T_c}{T_c}\right)^{-Y_1^1} \quad (4)$$

The results, shown in Table III, are qualitatively the same as for the variation (3), with the same standard deviation and quality of fits. In particular, the values of the exponent  $Y$  are the same:  $Y_1^1 = Y_1^0$ . The variation in  $T^{-1}$  does not influence obviously the behavior near  $T_c$ , but modifies the activation energy. We have for set  $\alpha$ :

$$\frac{E_1^1}{E} = 0.6 \pm 0.3, \quad \frac{Y_1^1}{Y} = \frac{Y_1^0}{Y} = 0.84 \pm 0.3,$$

and for set  $\alpha + \beta + \gamma$ :

$$\frac{E_1^1}{E} = 0.75 \pm 0.05, \quad \frac{Y_1^1}{Y} = \frac{Y_1^0}{Y} = 0.7 \pm 0.2.$$

The conclusion to be drawn following the study of this reorientation time is therefore that there is a weak anomaly of the  $T - T_c$  behavior, this anomaly being close to the anomaly of viscosity. The variation seems to be described best by Eq. (3).

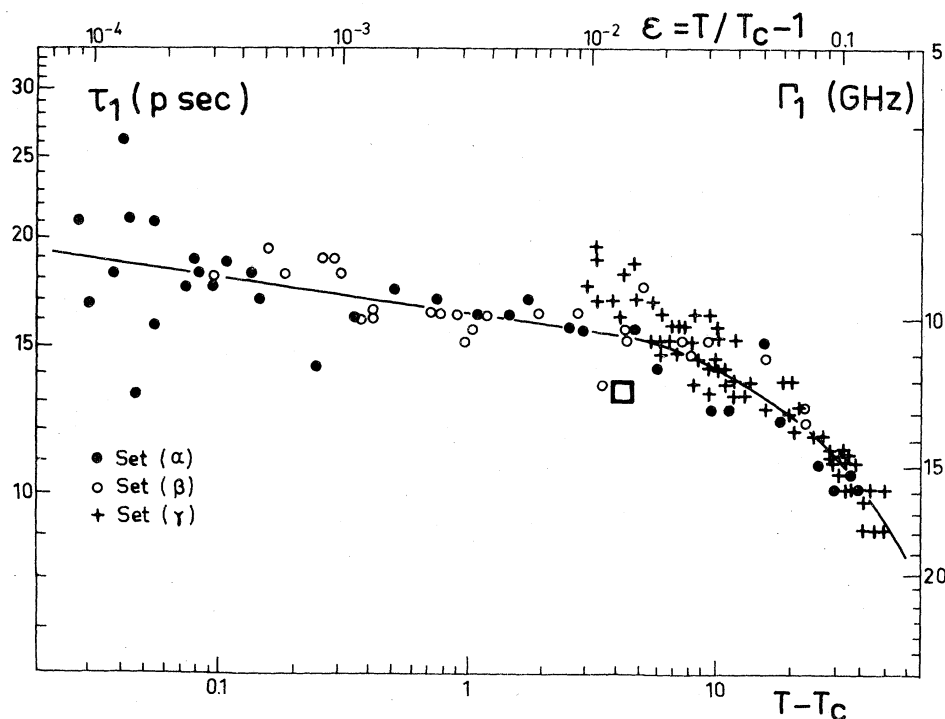


FIG. 5. Variation of line-width  $\tau_1$  vs  $T - T_c$ . The line is the fit to the expression:  $\tau_1 = \tau_1^0 \exp(E_1^0/kT) \cdot [(T - T_c)/T_c]^{-Y_1^0}$ . The square is the value inferred from measurements in a non critical mixture (see text).

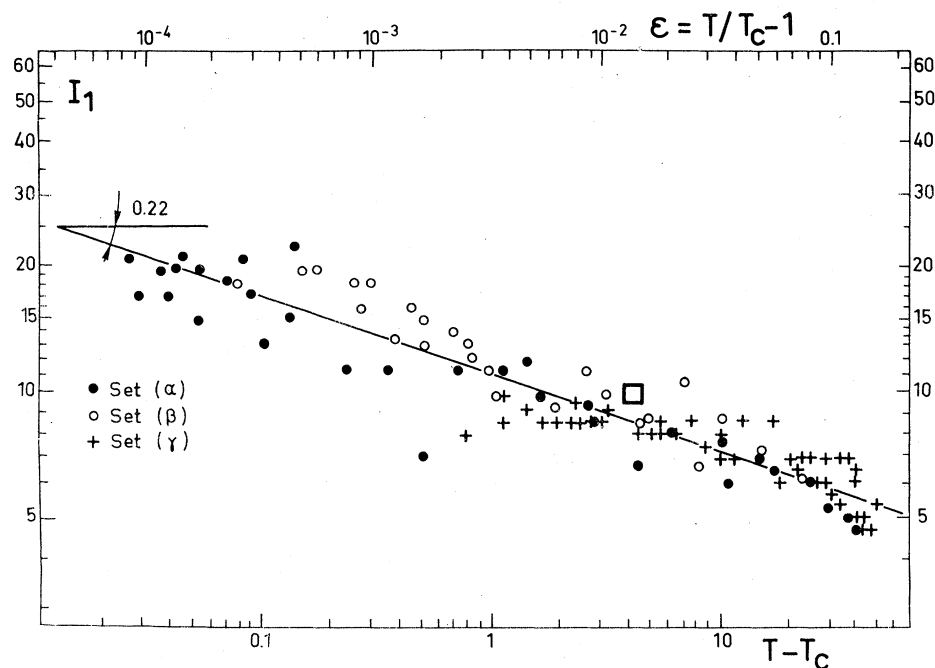


FIG. 6. Variation of intensity  $I_1$  vs  $T - T_c$ . The line corresponds to the variation:  $I_1 \propto (T - T_c)^{-\Omega}$ . The square is the value obtained in noncritical mixtures (see text).

### 3. Narrow line: Study of the intensity

As we have previously pointed out, the variation of the integral  $I_1$  of the narrow line (1) has been obtained by three different methods, according to the set of experimental results. They are compatible to within a multiplying constant with a power-law variation with an exponent  $\Omega \approx 0.22$  as shown in Fig. 6. More precisely, we performed a fit following the formula

$$I_1 = A_{\alpha, \beta, \gamma} (T - T_c)^{-\Omega}$$

The results are shown in Table IV, the value of  $\Omega$  ranging from 0.18 to 0.26 according to the set of experiments. The value

$$\Omega = 0.222 \pm 0.008$$

is obtained when fitting all sets.

Measurements of set  $\gamma$  have been referred to the intensity of line (1) in pure nitrobenzene, at the temperature of 24 °C<sup>12</sup>

TABLE IV. Fit to  $I_1 = X_1 \epsilon^{-\Omega}$ .  $\epsilon = (T - T_c)/T_c$ .

Set	$X_1$	$\pm \Delta X_1$	$\Omega$	$\pm \Delta \Omega$	$Q$	
$\alpha$	0.34	0.03	0.222	0.013	0.53	
$\beta$	0.34	0.035	0.26	0.02	0.75	
$\gamma$	2.2	0.15	0.18	0.02	0.70	
$\alpha + \beta + \gamma$	$\alpha, \beta$	0.36	0.02	0.222	0.008	0.85
	$\gamma$	2.0	0.7			

$$I_1(x = x_c, \text{critical})/I_1(x = 1) \approx 0.18, \quad T - T_c = 4 \text{ }^\circ\text{C}.$$

When comparing with noncritical mixtures of nitrobenzene, but at the same concentration<sup>5,6</sup> we find

$$I_1(x = x_c, \text{noncritical})/I_1(x = 1) \approx 0.22 \quad T = 24 \text{ }^\circ\text{C}.$$

Hence the ratio  $I_1(x = x_c, \text{critical})/I_1(x = x_c, \text{noncritical})$  can be evaluated. Its value  $\approx 0.82$  is nearly equal to one. Therefore the anomaly of the intensity is seen to be, as the anomaly of the linewidth, a weak anomaly in absolute size.

## IV. DISCUSSION

### A. Origin of the two lines

Several models are usually considered to explain a depolarized spectrum built up to two Lorentzian lines, one sharp and narrow, the other broad and weak:

(i) The "monomolecular model," which attributes these two lines to two rotational motions around different axes of the single molecule.<sup>27,28</sup> In noncritical mixtures, this model is shown not to be valid by the fact that the intensity of the narrow line does not vary linearly with the concentration of the anisotropic liquid, suggesting some orientation correlations.

(ii) The correlations have been taken into account by Keyes and Kivelson,<sup>29</sup> who obtained for

the narrow line

$$I_1 \sim N(1+fN), \quad \tau_1 = [(1+fN)/(1+gN)]\tau_s,$$

where  $f$  and  $g$  are the static and dynamic correlation coefficients,  $N$  is the number of anisotropic molecules per unit volume, and  $\tau_s$  is the reorientation time of a single molecule. In this model, however, only the case of a cylindrical symmetric molecule is considered, and the question concerning the origin of the second line is left open. Alms *et al.*<sup>6</sup> used this model and calculated  $\tau_s$  with the monomolecular model. They also suggested the presence of a second line due to reorientation around another axis of the same anisotropic molecule.

(iii) An alternative model has been elaborated by Quentrec<sup>30,31</sup> that accounts for the wide line by introducing a second local-order tensor, related to the short-range position correlations, while the treatment of the narrow line is very similar to that of Keyes and Kivelson.

A full discussion of this point would need a careful comparison of linewidths and intensities in different experimental cases and will be the subject of a future paper.<sup>21</sup> In this paper, we would rather focus our attention on the behavior of the narrow line at the critical concentration. We only note that all these models lead to a Lorentzian shape for the narrow line, i.e., refer to a diffusive process for the reorientation.

#### B. Anomaly of the intensity of the narrow line

In the monomolecular model at constant concentration, the intensity can vary only through the density or the local electric field. Now the density does not vary more than 5% throughout the considered temperature range. Even in pure nitrobenzene, the intensity varies much faster than the density at these temperatures but it varies roughly linearly with the temperature,<sup>2,25</sup> while we have here a power-law behavior. Refractive-index measurements near the critical point of a binary mixture<sup>32,33</sup> show that the combined effect of both factors remains very small. Therefore, this model is not consistent with the observed anomaly.

The correlation model leads to the following variation

$$I = I_0 N(1+fN),$$

where  $I_0$  and  $f$  can vary with the temperature. Since the factor  $fN$  is expected to be of order of unity from noncritical mixtures data,<sup>6</sup> a power-law behavior of  $f$  should not lead to a power-law behavior of  $I$ . However, experimental uncertain-

ties are large enough to prevent us from a clear-cut conclusion.

#### C. Anomaly of the width of the narrow line

The linewidth has been seen to exhibit the same behavior as the inverse macroscopic viscosity. This is compatible with the monomolecular theory in which each molecule rotates in a continuous medium, and the diffusion coefficient(s) is (are) related to the shear viscosity through the boundary conditions at the surface of the molecule (slip, stick, or other<sup>34,35</sup>). Although this model cannot explain the intensity variation, we can consider it as valuable for calculating the single-molecule rotation time  $\tau_s$ , as in Ref. (6). This hypothesis requires the ratio

$$(1+fN)/(1+gN)$$

to be temperature independent. Since  $f$  and  $g$  are very different in noncritical nitrobenzene mixtures ( $fN = 1.3$  and  $gN = 0.1 \pm 0.1$  in pure nitrobenzene), it is somewhat unlikely that they would vary with  $T - T_c$  in such a way that this ratio keeps constant. This is then another indication that  $f$  and  $g$  are constant—although the opposite proposition cannot be strictly discounted.

In other respects, Quentrec's theory relates this linewidth to a new formal coefficient  $\alpha_{33}$ ,  $\alpha_{11}$  being the viscosity, and therefore does not provide any new insight.

Nevertheless, in all cases, these results raise the question of the nature of the coupling between the low-frequency long-wavelength critical modes and a fast and short-ranged phenomenon like depolarized scattering. For instance, Carini *et al.*<sup>36</sup> have shown that the shear viscosity measured by usual methods exhibits a relaxation, a fact which clearly does not appear in our experiment, where a naive reasoning would lead to assert that the measuring frequency is about  $\Gamma \approx 10$  GHz and the typical length is the extent of local order, which cannot exceed 100 Å.

#### V. CONCLUSION

In order to try to answer the questions concerning the existence of two lines in the high-frequency depolarized spectrum of the critical mixture of nitrobenzene and *n* hexane, and the variations of their linewidths and intensities near the critical point, we set up a very high contrast and high-resolution Fabry-Perot interferometer in double passed arrangement and with two free spectral ranges.

Two lines are visible. One is broad and has a very weak spectral intensity so that it could not

be studied accurately. The other is narrow and intense and could be studied in the range  $T - T_c = 0.026 - 50^\circ\text{C}$ . The wide line is 15 times wider and 7 times less intense than the narrow line at  $T - T_c = 1^\circ\text{C}$ .

The width of the narrow line is seen to behave like the inverse of the macroscopic shear viscosity, in particular it exhibits a weak anomaly in  $(T - T_c)^Y$ , where  $Y \approx 0.04$ . The intensity of this line also shows a divergence which can be ex-

pressed in the form  $(T - T_c)^{-\Omega}$  with exponent  $\Omega \approx 0.2$ .

The existing theories do not provide an adequate frame for the discussion of these results which raise many questions, mainly concerning the nature of the coupling between the order parameter and the orientation fluctuations. New experiments are currently underway in order to try to understand the origin of the anomalies in both the linewidth and intensity.

- <sup>1</sup>D. A. Pinnow, S. J. Candau, and T. A. Litovitz, *J. Chem. Phys.* **49**, 347 (1968).
- <sup>2</sup>E. Zamir, N. Gershon, and A. Ben-Reuven, *J. Chem. Phys.* **55**, 3397 (1971).
- <sup>3</sup>S. J. Bertucci, A. K. Burnham, G. R. Alms, and W. H. Flygare, *J. Chem. Phys.* **66**, 605 (1977).
- <sup>4</sup>J. Rouch, J. P. Chabrat, L. Letamendia, A. Marcou, and C. Vaucamps, *Acta Phys. Pol. A* **50**, 503 (1976).
- <sup>5</sup>D. J. Coumou, J. Hijmans, and E. L. Mackor, *Trans. Faraday Soc.* **60**, 2244 (1964).
- <sup>6</sup>G. R. Alms, D. R. Bauer, J. I. Brauman, and R. Pecora, *J. Chem. Phys.* **59**, 5310 (1973).
- <sup>7</sup>A. K. Atakhodzhaev, L. M. Kashaeva, L. M. Sabirov, V. S. Starunov, T. M. Utarova, and I. L. Fabelinskii, *JETP Lett.* **17**, 65 (1973).
- <sup>8</sup>I. L. Fabelinskii, V. S. Starunov, A. K. Atakhodzhaev, L. M. Sabirov, and T. M. Utarova, *Opt. Commun.* **15**, 432 (1975).
- <sup>9</sup>I. L. Fabelinskii, G. I. Kolesnikov, V. J. Sheiner, and V. S. Starunov, *Phys. Lett. A* **59**, 408 (1976); I. L. Fabelinskii, G. I. Kolesnikov, and V. S. Starunov, *Opt. Commun.* **20**, 130 (1977).
- <sup>10</sup>I. L. Fabelinskii, V. S. Starunov, A. K. Atakhodzhaev, L. M. Sabirov, and J. M. Utarova, *Opt. Commun.* **20**, 135 (1977).
- <sup>11</sup>I. M. Aref'ev, *Opt. Commun.* **10**, 277 (1974).
- <sup>12</sup>D. Beysens, A. Bourgou, and G. Zalczer, *Opt. Commun.* **15**, 436 (1975).
- <sup>13</sup>D. Beysens, S. H. Chen, J. P. Chabrat, L. Letamendia, J. Rouch, and P. Vaucamps, *J. Phys. (Paris) Lett.* **38**, L203 (1977).
- <sup>14</sup>D. Beysens and G. Zalczer, *Opt. Commun.* **22**, 236 (1977).
- <sup>15</sup>S. H. Chen and N. Polonski, *Opt. Commun.* **1**, 64 (1969).
- <sup>16</sup>C. C. Lai and S. H. Chen, *Phys. Rev. Lett.* **29**, 401 (1972).
- <sup>17</sup>C. C. Lai, S. H. Chen, *Phys. Lett. A* **41**, 259 (1972).
- <sup>18</sup>D. Beysens, A. Bourgou, and H. Charlin, *Phys. Lett. A* **53**, 236 (1975).
- <sup>19</sup>D. Beysens, A. Bourgou, and G. Zalczer, *J. Phys. (Paris) Colloq. C* **1**, 225 (1976).
- <sup>20</sup>D. Beysens, G. Zalczer, *Phys. Rev.* **A15**, 765 (1977).
- <sup>21</sup>D. Beysens and G. Zalczer (unpublished).
- <sup>22</sup>D. Beysens and G. Zalczer, *Opt. Commun.* **23**, 142 (1977).
- <sup>23</sup>V. Puglielli and N. Ford, *Phys. Rev. Lett.* **25**, 143 (1970).
- <sup>24</sup>M. Tournarie, *J. Phys. (Paris)* **30**, 47 (1969).
- <sup>25</sup>G. I. A. Stegeman and B. P. Stoicheff, *Phys. Rev. A* **7**, 1160 (1973).
- <sup>26</sup>B. Simic-Glavaski and D. A. Jackson, *J. Phys. (Paris) Colloq.* **33**, C1-183 (1972).
- <sup>27</sup>E. N. Ivanov, *JETP* **18**, 1041 (1975).
- <sup>28</sup>R. Pecora, *J. Chem. Phys.* **49**, 1036 (1968).
- <sup>29</sup>T. Keyes and D. Kivelson, *J. Chem. Phys.* **56**, 1057 (1972).
- <sup>30</sup>B. Quentrec, *J. Phys. (Paris)* **37**, 1255 (1976).
- <sup>31</sup>B. Quentrec, *Phys. Rev.* **A15**, 1304 (1977).
- <sup>32</sup>C. L. Hartley, D. T. Jacobs, R. C. Mockler, and W. J. O'Sullivan, *Phys. Rev. Lett.* **33**, 1129 (1974).
- <sup>33</sup>D. T. Jacobs, D. J. Anthony, R. C. Mockler, and W. J. Sullivan, *Chem. Phys.* **20**, 219 (1977).
- <sup>34</sup>C. M. Hu and R. Zwanzig, *J. Chem. Phys.* **60**, 4354 (1974).
- <sup>35</sup>D. Hoel and D. Kivelson, *J. Chem. Phys.* **62**, 1323 (1975).
- <sup>36</sup>G. Carini Jr., G. Maisano, P. Migliardo, and F. Wanderlingh, *Phys. Rev. A* **11**, 1755 (1975).